International Journal on Magnetic Particle Imaging
Vol 3, No 1, Article ID 1703013, 5 Pages

Infinite Science Publishing

Research Article

Experimental Validation of the Selection Field of a Rabbit-Sized FFL Scanner

Anna Bakenecker*· Thomas Friedrich· Anselm von Gladiss· Matthias Graeser· Jan Stelzner· Thorsten M. Buzug*

Institute of Medical Engineering, University of Lübeck, Lübeck, Germany
*Corresponding author, email: {bakenecker, buzug}@imt.uni-luebeck.de

Received 25 November 2016; Accepted 25 February 2017; Published online 23 March 2017

Abstract

There are two different field topologies in magnetic particle imaging which enable the spatial encoding of the signal. Scanners using a field-free line (FFL) are promising regarding their sensitivity, because the low field volume is larger compared to a field-free point (FFP) and therefore, more particles contribute to the signal. A rabbit-sized FFL scanner with a bore diameter of 180 mm was presented in 2014. After planning and assembling the scanner an experimental validation of the designated field topology of the selection field is presented. With a hall probe the field topologies of the z-gradient coil and the two quadrupole coils forming together the selection field of the scanner were investigated. These magnetic field measurements show the expected field topologies: an FFP formed by the z-gradient coil and an FFL parallel to the bore of the scanner formed by each quadrupole coil. From these measurements the field gradients were calculated and approximated towards their designated currents. The results are in good agreement with the expected field gradients. Since power losses in the shielding occur for higher frequencies and the power transmission of the transformer is problematic for low frequencies, the best suitable frequency for rotating the FFL was evaluated. 20 Hz is chosen as it represents the best compromise between transformer performance and power loss in the shielding.

I. Introduction

In 2008, the theoretical concept of using a field-free line (FFL) [1] instead of using a field-free point (FFP) to spatially encode the receive signal of a Magnetic Particle Imaging (MPI) scanner [2–7] was introduced. By using an FFL, a gain of sensitivity by a factor of 3.6 and faster imaging is predicted, caused by a larger low-field volume and more particles contribute to the signal [1, 8]. In 2010, the first experimental setup for generating a static FFL was presented by Knopp et al. [9]. Later, a scanner with an inner diameter of 50 mm, which consists of four selection field coil pairs was introduced by Erbe et al. [10]. With this setup the proof of a rotating and translating FFL was provided. However, the high electrical power consumption as well as the small field gradient, which would result into low image resolution, were drawbacks of this scanner setup. An optimization was presented by Erbe et al. [11]. A special curved rectangular shape of the selection field coils were predicted to provide a better field homogeneity by a factor of five and less power consumption by almost a factor of four. In 2013 the introduced scanner setup realized the curved rectangular shape of the selection field coils and reached a field gradient of 1.5 Tm^{-1} and a suitable power loss [12], which can be seen as the small prototype of the rabbit-sized FFL scanner.

The field generator of the rabbit sized FFL scanner consists of two pairs of saddle-shaped drive-field coils.

The designated excitation frequency is at 25 kHz. In order to shield the selection field coils against the high frequency of the drive field and to prevent coupling, a copper shield is assembled between the drive-field coils and the selection field coils [13]. The selection field coils consist of a Maxwell coil for the z-gradient and two pairs of saddle-shaped quadrupole coils (see Fig. 1).

Figure 1: The field generator of the rabbit-sized FFL scanner. Left: It consists of two pairs of drive field coils (red), a Maxwell coil (blue) and two pairs of selection field quadrupole coils (green). Right: The realized setup at which the outermost quadrupole coil can be seen.

With a direct current of 800 A for the z-gradient coil a field gradient of 0.8 Tm^{-1} is aimed for. The designated currents for the quadrupole coils named Q_0 and Q_{45} are 430 A_{RMS} and 480 A_{RMS}, respectively leading to a field gradient of 0.5 Tm^{-1}. The planned frequency for the rotation of the FFL was 100 Hz [14], however experiments show that this would lead to high power losses in the shielding. Therefore, a lower frequency is preferable. A tradeoff between the aforementioned disadvantages and a good imaging acquisition rate as well as the technical feasibility is aimed. Technical feasibility is meant to be the power transmission of the transformer needed for current amplification behind the power amplifiers and the capacitors for power factor correction.

II. Material and Methods

Experiments validating the field topologies in a DC steady state were performed. In a second step the frequency of FFL rotation was determined.

II.I. Magnetic Field Topology

A hall probe and Gaussmeter (Lake Shore, Model 460) were used to measure the magnetic field within a volume of 6×6×6 cm^3 and a 7×7×7 grid, which is equal to a measurement point every 1 cm. A DC current of 30 A was applied to the Maxwell coil and to each of the quadrupole coils.

II.II. Rotation Frequency

For the designated selection field path (see Fig. 2), the best suitable frequency was investigated. First, the coil resistance was measured via an impedance analyzer (Keysight, E4990A) having a measurement range starting at 20 Hz for the aimed frequency range determining the power loss of the shielding. Second, the technical feasibility was validated by connecting a load of 25 mΩ by four power resistors of 100 mΩ each instead of the quadrupole coils to the designated power amplifiers (AE Techron 7796) and observing the current on the primary and the secondary side of the transformer (Rist, EN61558). One amplifier provides a power of 5 kW and a maximum voltage of 100 V when the optimal load of the amplifier is 2 Ω. Up to 400 A_{RMS} (on the secondary side) was applied in short pulses due to heat production in the resistors. Frequencies between 10 Hz and 100 Hz have been tested.

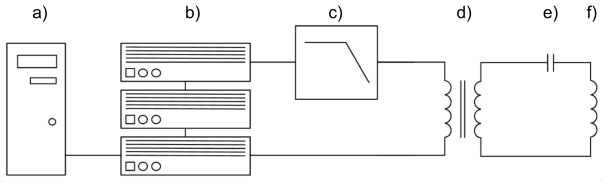

Figure 2: Quadrupole Tx-path with signal generator (a), amplifiers (b), low pass filter (c), transformer (d), power factor correction (e) and selection field coil (f) [15].

III. Results

III.I. Magnetic Field Topology

The measurement results of the magnetic field topologies can be seen in Fig. 3. An FFP is formed by the Maxwell coil and an FFL along the long axis of the scanner by each quadrupole coil. The magnetic field strength and the field gradient of an ideal Maxwell coil can be calculated according to

$$B_z = \frac{\mu_0 I R^2 N}{2\sqrt{R^2+\left(\frac{d}{2}-z\right)^2}^3} - \frac{\mu_0 I R^2 N}{2\sqrt{R^2+\left(\frac{d}{2}+z\right)^2}^3} \tag{1}$$

$$\frac{\mathrm{d}B_z}{\mathrm{d}z} = 0.6413\mu_0 N I R^{-2}. \tag{2}$$

With a coil radius of $R = 0.174$ m, number of windings $N = 40$, μ_0 the magnetic field constant and an applied current of $I = 30$ A for an ideal Maxwell coil a field gradient of $\mathrm{d}B/\mathrm{d}z = 0.032\ \mathrm{Tm}^{-1}$ is expected. The measured field gradient according to Fig. 3a) is 0.028 Tm^{-1}. A linear approximation towards the designated current of 800 A would lead to a field gradient of 0.76 Tm^{-1}. The calculation for an ideal Maxwell coil predicts a field gradient of 0.85 Tm^{-1}. The measured field gradient for both

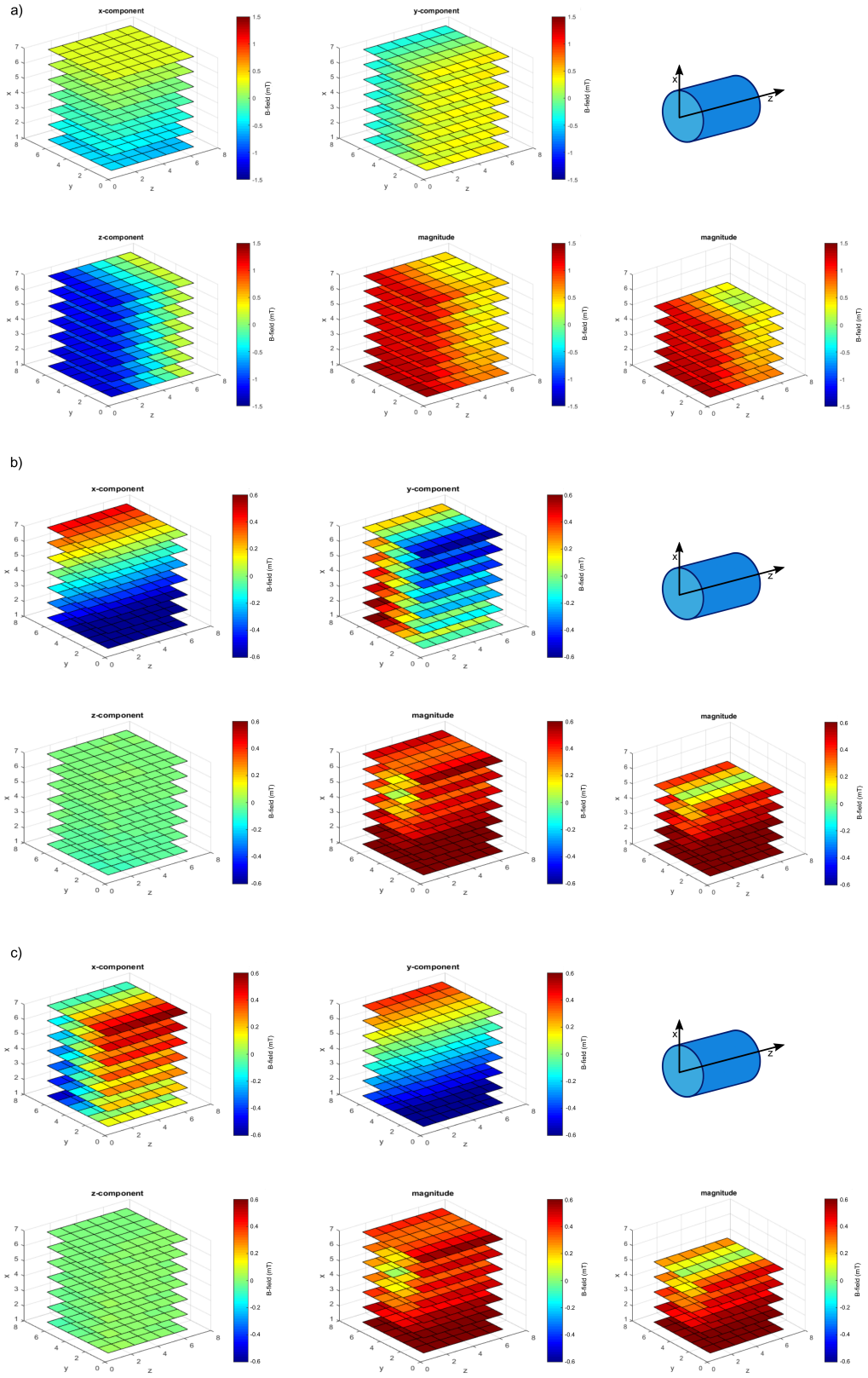

Figure 3: Measured magnetic field topologies with a hall probe. a) z-gradient coil, b) 0° quadrupole coil and c) 45° quadrupole coil. The x- y- and z-component as well as the magnitude of the magnetic field are shown.

10.18416/ijmpi.2017.1703013

quadrupole coils according to Fig. 3b) and Fig. 3c) is 0.015 $\mathrm{Tm^{-1}}$. A linear approximation towards the designated currents of 430 $\mathrm{A_{RMS}}$ and 480 $\mathrm{A_{RMS}}$ leads to a field gradient of 0.45 $\mathrm{Tm^{-1}}$. A field gradient of 0.5 $\mathrm{Tm^{-1}}$ was theoretically aimed for the quadrupoles.

III.II. Rotation frequency

The measured resistance of the quadrupole coils increases with the frequency. Since the actual resistance stays constant, this increase refers to an increasing power loss in the shielding. An increase of the coil resistance of 79 % for the quadrupole $\mathrm{Q_0}$ and 54 % for $\mathrm{Q_{45}}$ from 20 Hz to 100 Hz was observed. The measurement results can be found in Fig. 4.

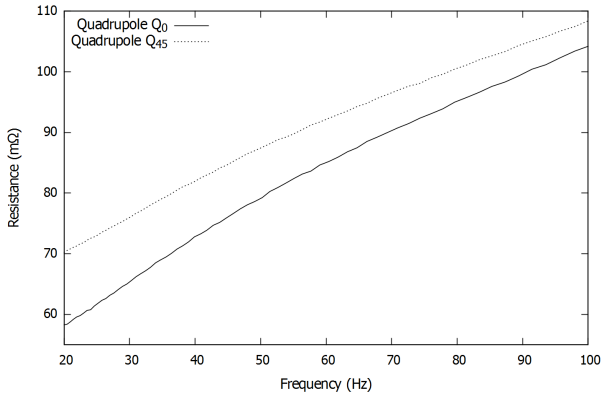

Figure 4: Resistances of the quadrupoles $\mathrm{Q_0}$ and $\mathrm{Q_{45}}$ over frequency measured with an impedance analyzer (Keysight, E4990A) in a range of 20 Hz to 100 Hz.

The observed current amplitudes on the primary and secondary side of the transformer stayed constant with the transformation factor of eleven from approximately 20 Hz on. So choosing 20 Hz as the selection-field rotation frequency seems to be a good compromise between power loss in the shielding and well performed power transmission of the transformer.

Then the equation $X_\mathrm{L} + X_\mathrm{C} = 0$ should hold for compensating the inductive reactance. The needed capacitance is then

$$C_S = \frac{1}{\omega^2 L} = \begin{cases} 175\,\mathrm{mF}, & \text{for } \mathrm{Q_0} \\ 146\,\mathrm{mF}, & \text{for } \mathrm{Q_{45}} \end{cases} \tag{3}$$

with the measured inductances of 363 μH and 434 μH, respectively. With two AE Techron 7796 power amplifiers in series for each quadrupole coil a maximum continuous power output of 10 kW is available. Together, the amplifiers optimum load is $R_\mathrm{Opt} = 4\,\Omega$. The transformer voltage ratio is given by

$$\alpha = \frac{U_P}{U_S} = \frac{N_P}{N_S}, \tag{4}$$

with N being the number of windings and P the primary and S the secondary side of the transformer. Assuming that

$$P_P = U_P I_P = U_S I_S = P_S \tag{5}$$

holds, the transformer voltage ratio can be calculated via

$$\alpha^2 = \frac{Z_P}{Z_S} = \frac{R_\mathrm{Opt}}{R_\mathrm{Quad}} \tag{6}$$

with R_Quad being the resistances of the quadrupole coils, which are given in Tab. 1. With this, a transformer voltage ratio α of 8.3 and 7.6, respectively can be calculated. This leads to a maximum voltage on the secondary side of 24.1 V and 26.3 V and a maximum current of 413 A and 375 A, respectively. These calculations were performed according to [15]. An overview on the designated settings for the quadrupole coils are given in Tab. 1.

Table 1: Specifications of the quadrupole coils $\mathrm{Q_0}$ and $\mathrm{Q_{45}}$.

	$\mathbf{Q_0}$	$\mathbf{Q_{45}}$
Current (desginated)	430 $\mathrm{A_{RMS}}$	480 $\mathrm{A_{RMS}}$
Current (achievable)	413 $\mathrm{A_{RMS}}$	375 $\mathrm{A_{RMS}}$
Resistance $\mathbf{R_{Quad}}$ at 20 Hz	58 mΩ	70 mΩ
Voltage (secondary side)	24.1 V	26.3 V
Inductance at 20 Hz	363 μH	434 μH
Capacitance C_S	174 mF	146 mF
Transformer voltage ratio	8.3	7.6

IV. Conclusion and Outlook

The magnetic field measurements show the expected field topologies. A linear approximation towards the designated currents are in good agreement with the theoretically expected field gradient of 0.8 $\mathrm{Tm^{-1}}$ for the z-gradient and 0.5 $\mathrm{Tm^{-1}}$ for the quadrupoles.

Since severe power losses occur for higher frequencies a lower frequency than the former designated one needs to be chosen. The transformer, which is actually designated for 100 Hz, performed well from 20 Hz on. Therefore a rotation frequency of the FFL is chosen to be 20 Hz, because the power losses in the shielding are kept as low as possible and the transformer performed the designated power transmission from primary to secondary side. However, by using two AE Techron 7796 amplifiers for each quadrupole coil the designated currents cannot be achieved. With the installed transformer one can only achieve a maximum current of 313 A and 260 A, respectively. Installing new transformers having the calculated and here presented transformation factors would also lead to lower currents (413 A and 375 A) and therefore lower field gradients than predicted (430 A and 480 A), when using a frequency of 20 Hz instead of 100 Hz. One

10.18416/ijmpi.2017.1703013

would need three amplifiers for the Q_0 and four amplifiers for the Q_{45} quadrupole coil in order to reach the designated currents when using a frequency of 20 Hz. The resulting lower field gradient will reduce the resolution of the scanner. Two transformers as well as the capacitors for power factor correction need to be installed according to the calculations from above. Moreover, some low pass feedthrough filters need to be installed in order to eliminate any disturbances from outside the shielding cabin. Then, the selection field can be driven towards its designated settings.

Acknowledgement

Founding by the German Research Foundation (DFG) under Grant Number BU 1436/7-1 is gratefully acknowledged.

References

[1] J. Weizenecker, B. Gleich, and J. Borgert. Magnetic particle imaging using a field free line. *J. Phys. D: Appl. Phys.*, 41(10):105009, 2008. doi:10.1088/0022-3727/41/10/105009.

[2] B. Gleich and J. Weizenecker. Tomographic imaging using the nonlinear response of magnetic particles. *Nature*, 435(7046):1214–1217, 2005. doi:10.1038/nature03808.

[3] B. Gleich, J. Weizenecker, and J. Borgert. Experimental results on fast 2D-encoded magnetic particle imaging. *Phys. Med. Biol.*, 53 (6):N81–N84, 2008. doi:10.1088/0031-9155/53/6/N01.

[4] P. Vogel, M. A. Rückert, P. Klauer, W. H. Kullmann, P. M. Jakob, and V. C. Behr. Traveling Wave Magnetic Particle Imaging. *IEEE Trans. Med. Imag.*, 33(2):400–407, 2014. doi:10.1109/TMI.2013.2285472.

[5] T. Wawrzik, C. Kuhlmann, F. Ludwig, and M. Schilling. Scanner setup and reconstruction for three-dimensional magnetic particle imaging. In *SPIE Medical Imaging*, 2013. doi:10.1117/12.2006392.

[6] P. W. Goodwill, K. Lu, B. Zheng, and S. M. Conolly. An x-space magnetic particle imaging scanner. *Rev. Sci. Instrum.*, 83(3):033708, 2012. doi:10.1063/1.3694534.

[7] J. Franke, U. Heinen, H. Lehr, A. Weber, F. Jaspard, W. Ruhm, M. Heidenreich, and V. Schulz. System Characterization of a Highly Integrated Preclinical Hybrid MPI-MRI Scanner. *IEEE Trans. Med. Imag.*, 35(9):1993–2004, 2016. doi:10.1109/TMI.2016.2542041.

[8] P. W. Goodwill, J. J. Konkle, B. Zheng, E. U. Saritas, and S. M. Conolly. Projection X-Space Magnetic Particle Imaging. *IEEE Trans. Med. Imag.*, 31(5):1076–1085, 2012. doi:10.1109/TMI.2012.2185247.

[9] T. Knopp, M. Erbe, T. F. Sattel, S. Biederer, and T. M. Buzug. Generation of a static magnetic field-free line using two Maxwell coil pairs. *Appl. Phys. Lett.*, 97(9):092505, 2010. doi:10.1063/1.3486118.

[10] M. Erbe, T. Knopp, T. F. Sattel, S. Biederer, and T. M. Buzug. Experimental generation of an arbitrarily rotated field-free line for the use in magnetic particle imaging. *Med. Phys.*, 38(9):5200–5207, 2011. doi:10.1118/1.3626481.

[11] M. Erbe, T. F. Sattel, and T. M. Buzug. Improved field free line magnetic particle imaging using saddle coils. *Biomed. Tech. / Biomed. Eng.*, 58(6):577–582, 2013. doi:10.1515/bmt-2013-0030.

[12] M. Weber, M. Erbe, K. Bente, T. F. Sattel, and T. M. Buzug. Scanner Construction for a Dynamic Field Free Line in Magnetic Particle Imaging. In *Biomed. Tech.*, volume 58, 2013. doi:10.1515/bmt-2013-4259.

[13] G. Bringout, M. Ahlborg, M. Graeser, C. Kaethner, J. Stelzner, W. Tenner, H. Wojtczyk, and T. M. Buzug. Shielded Drive Coils for a Rabbit Sized FFL Scanner. In *International Workshop on Magnetic Particle Imaging*, 2014.

[14] G. Bringout, J. Stelzner, M. Ahlborg, A. Behrends, K. Bente, C. Debbeler, A. von Gladiss, K. Graefe, M. Graeser, C. Kaethner, S. Kaufmann, K. Lüdtke-Buzug, H. Medimagh, W. Tenner, M. Weber, and T. M. Buzug. Concept of a rabbit-sized FFL-scanner. In *International Workshop on Magnetic Particle Imaging*, 2015. doi:10.1109/IWMPI.2015.7107032.

[15] A. Behrends, M. Graeser, J. Stelzner, and T. M. Buzug. Signal Chain Optimization in Magnetic Particle Imaging. In *Biomed. Tech.*, 2014. doi:10.1515/bmt-2014-5008.

